

RESEARCH ARTICLE

Nicotinic acid receptor agonists impair myocardial contractility by energy starvation

William D. Watson¹ | Kerstin N. Timm² | Andrew J. Lewis¹ | Jack J. J. Miller^{1,2,3} | Yaso Emmanuel² | Kieran Clarke² | Stefan Neubauer¹ | Damian J. Tyler² | Oliver J. Rider¹

¹Department of Cardiovascular Medicine, Oxford Centre for Clinical Magnetic Resonance Research, University of Oxford, Oxford, UK

²Department of Physiology, Anatomy and Genetics, University of Oxford, Oxford, UK

³Department of Physics, University of Oxford, Oxford, UK

Correspondence:

William D. Watson, Oxford Centre for Clinical Magnetic Resonance Research, Department of Cardiovascular Medicine, Radcliffe Department of Medicine, University of Oxford, Level 6, West Wing, John Radcliffe Hospital, Headington, Oxford OX3 9DU, UK.
Email: william.watson@st-annes.ox.ac.uk

Funding information

This work was supported by the British Heart Foundation. WW is supported by a British Heart Foundation Clinical Research Training Fellowship (FS/17/48/32907). KNT is supported by a British Heart Foundation Immediate Postdoctoral Basic Science Research Fellowship (FS/16/7/31843). DJT is supported by a British Heart Foundation Senior Fellowship (FS/19/18/34252). OR is supported by a British Heart Foundation Intermediate Fellowship (FS FS/16/70/32157). JJM

Abstract

Nicotinic acid receptor agonists have previously been shown to cause acute reductions in cardiac contractility. We sought to uncover the changes in cardiac metabolism underlying these alterations in function. In nine humans, we recorded cardiac energetics and function before and after a single oral dose of nicotinic acid using cardiac MRI to demonstrate contractile function and Phosphorus-31 (³¹P) magnetic resonance spectroscopy to demonstrate myocardial energetics. Nicotinic Acid 400 mg lowered ejection fraction by 4% ($64 \pm 8\%$ to $60 \pm 7\%$, $P = .03$), and was accompanied by a fall in phosphocreatine/ATP ratio by 0.4 (2.2 ± 0.4 to 1.8 ± 0.1 , $P = .04$). In four groups of eight Wistar rats, we used pyruvate dehydrogenase (PDH) flux studies to demonstrate changes in carbohydrate metabolism induced by the nicotinic acid receptor agonist, Acipimox, using hyperpolarized Carbon-13 (¹³C) magnetic resonance spectroscopy. In rats which had been starved overnight, Acipimox caused a fall in ejection fraction by 7.8% (67.5 ± 8.9 to 60 ± 3.1 , $P = .03$) and a nearly threefold rise in flux through PDH (from 0.182 ± 0.114 to 0.486 ± 0.139 , $P = .002$), though this rise did not match pyruvate dehydrogenase flux observed in rats fed carbohydrate rich chow (0.726 ± 0.201). In fed rats, Acipimox decreased pyruvate dehydrogenase flux (to 0.512 ± 0.13 , $P = .04$). Concentration of plasma insulin fell by two-thirds in fed rats administered Acipimox (from 1695 ± 891 ng/L to 550 ± 222 ng/L, $P = .005$) in spite of glucose concentrations remaining the same. In conclusion, we demonstrate that nicotinic acid receptor agonists impair cardiac contractility associated with a decline in cardiac energetics and show that the mechanism is likely a combination of

Abbreviations: AMARES, advanced method for accurate, robust and efficient spectral fitting; ATP, adenosine triphosphate; CMR, cardiac magnetic resonance; ¹³C, carbon-13; [1-¹³C]pyruvate, pyruvate labeled with 13-carbon in the 1st carbon position; CSI, Chemical Shift Imaging; ELISA, enzyme-linked immunosorbent assay; FDG-PET, fluorodeoxyglucose positron emission tomography; FFA, free fatty acid(s); FLASH, fast low angle shot magnetic resonance imaging; LDH, lactate dehydrogenase; LV, left ventricular; LVEF, left ventricular ejection fraction; MR, magnetic resonance; MRI, magnetic resonance imaging; MRS, magnetic resonance spectroscopy; ³¹P, phosphorous-31; PCr, phosphocreatine; PCr/ATP, ratio of phosphocreatine to ATP (derived from ³¹P MR spectra); PDH, pyruvate dehydrogenase; PET, positron emission tomography; PPAR, peroxisome proliferator activated receptor; SSFP, steady state free precession; TE, echo time; TR, repetition time.

This is an open access article under the terms of the Creative Commons Attribution License, which permits use, distribution and reproduction in any medium, provided the original work is properly cited.

© 2020 The Authors. *The FASEB Journal* published by Wiley Periodicals LLC on behalf of Federation of American Societies for Experimental Biology

would like to acknowledge an EPSRC Doctoral Prize Fellowship (ref. EP/M508111/1) and Novo Nordisk Postdoctoral Research Fellowship run in conjunction with the University of Oxford

reduced fatty acid availability and a failure to upregulate carbohydrate metabolism, essentially starving the heart of fuel.

KEYWORDS

cardiac metabolism, nicotinic acid, ^{31}P MR spectroscopy, hyperpolarized ^{13}C pyruvate

1 | INTRODUCTION

In the normal adult heart, most (60%-90%) of myocardial ATP is generated by mitochondrial β -oxidation of free fatty acids, with a smaller (10%-40%) contribution from glucose oxidation.¹ However, the heart alters substrate preference depending on metabolic conditions, accommodating increased fatty acid and ketone availability when fasting or increased glucose availability when feeding with no change in cardiac function.² The relative proportions of substrates metabolized are important, as fatty acid metabolism provides less energy per unit oxygen consumed,³ linking substrate selection to ATP production and cardiac performance,^{4,5} which makes modulation of metabolism a potential therapeutic target.

Nicotinic acid (and its derivative, Acipimox) act on the GPR109a receptor, blocking lipolysis in adipocytes via adenylyl cyclase inhibition,⁶ causing a fall in circulating fatty acids. This has been shown to increase glucose metabolism via the Randle cycle, where low levels of fat metabolism activate glucose metabolism via increasing glucose uptake, phosphofructokinase, and pyruvate dehydrogenase (and vice-versa, where excess beta oxidation causes acetyl-CoA accumulation, inhibiting pyruvate dehydrogenase).^{7,8} This stimulation of myocardial glucose uptake has led to their use in FDG-PET, where Acipimox has been shown to increase glucose uptake to a similar extent as a euglycemic insulin clamp.^{9,10}

The putative improvement in myocardial efficiency by promoting glucose metabolism over fatty acid metabolism has led to nicotinic acid receptor agonists being proposed as heart failure treatments. However, heart failure trials to date have not shown any benefit, with no improvement in ventricular function over 28 days¹¹ and mechanistic studies have shown short-term reductions in systolic function.¹²⁻¹⁴ The mismatch between the suggested benefits of nicotinic acid receptor agonists and their adverse effects on the myocardium is paradoxical.

We hypothesized that the acute depression of systolic function following nicotinic acid receptor agonists is due to reduced ATP production resulting from altered cardiac substrate metabolism. To investigate this, we first used human cardiac magnetic resonance imaging (MRI) and ^{31}P magnetic resonance spectroscopy (MRS) to document the effect of nicotinic acid receptor agonists on fatty acid availability, myocardial energetics and cardiac function. We then used magnetic resonance imaging and hyperpolarized Carbon-13

(^{13}C) MRS in rodents following Acipimox, to investigate surrogates of glucose metabolism following nicotinic acid receptor agonism.

2 | MATERIALS AND METHODS

2.1 | Human study

This prospective observational study of healthy volunteers was approved by the National Research Ethics Service (LREC no. 06/Q1607/38) and conformed to the principles outlined in the Declaration of Helsinki. Nine adult participants in this study were recruited from the Oxfordshire area on a voluntary basis by poster advertisement. Potential participants were screened briefly on the telephone, and then, fully assessed in the Department of Cardiovascular Medicine for exclusion criteria. Written informed consent was obtained from all participants. The study is summarized in Figure 1.

2.1.1 | Exclusion criteria

Participants were excluded if they were taking cardiovascular medication, had a current or past smoking habit, were diabetic (fasting serum glucose > 7.0 mM), hyperlipidemic (cholesterol > 6.5 mM), hypertensive (>140/90 mmHg), or had an abnormal electrocardiograph. Participants with a history or clinical evidence of heart failure, obstructive sleep apnea, valvular or congenital heart disease, or contraindication to MR scanning were also excluded.

2.1.2 | Anthropometric and biochemical measurements

Heights and weights were measured using a digital station (Seca, UK) and were used to calculate Body Mass Index (BMI). Blood pressure was recorded as an average of three supine measures taken over 10 minutes (DINAMAP-1846-SX, Critikon Corp). Venous blood was drawn during the experiments and sent for biochemical analysis of β -hydroxybutyrate, insulin, glucose, and free fatty acids (FFA, ABX Pentra System).

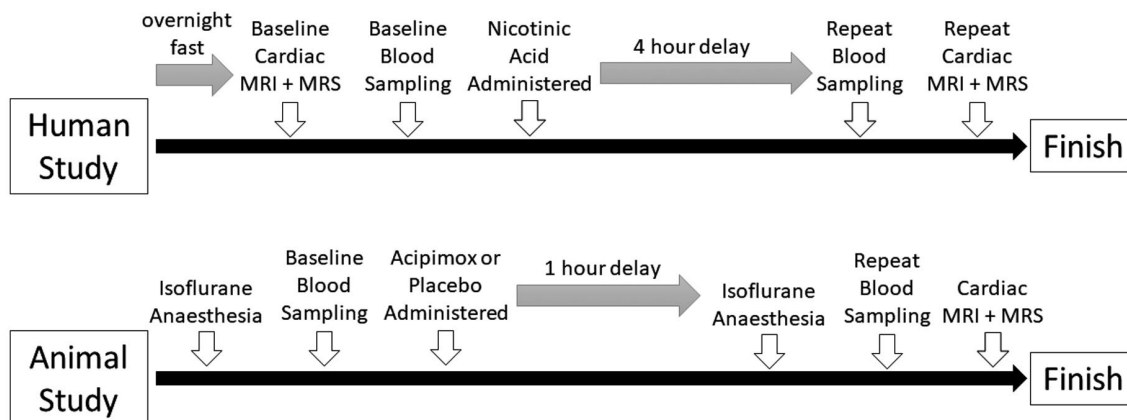


FIGURE 1 Study procedures

2.1.3 | Substrate modulation

Subjects were requested to fast from midnight the previous day and attend at 8 AM for their baseline measurements. Reduction of circulating free fatty acids (FFAs) was accomplished with a single 400 mg oral dose of nicotinic acid (Niaspan®, Abbot, UK). MRI and MRS, and blood samples for glucose, β -hydroxybutyrate, FFA, and insulin were taken at baseline and during the FFA-lowering experiment prior to scanning at 4 hours.

2.1.4 | Left ventricular imaging

All cardiac magnetic resonance (CMR) scans for the assessment of the left ventricle were performed on a 1.5 T MR system (Siemens, Germany). Images for ventricular volumes and diastolic function were acquired using a steady state free precession (SSFP) sequence with an echo time (TE) of 1.5 ms, a repetition time (TR) of 3.0 ms, in plane resolution $1.5 \text{ mm}^2 \times 1.5 \text{ mm}^2$, temporal resolution 47.84 ms, flip angle 60° , as previously described.¹⁵ All imaging was performed supine, retrospectively cardiac gated and acquired during end-expiratory breath-hold. All analysis was performed using cmr42® (Circle Cardiovascular Imaging Inc, Calgary, Canada) as previously described.¹⁶ Global peak circumferential diastolic strain rates were determined by feature tracking analysis. Endocardial and epicardial left ventricular (LV) contours were drawn on the LV short axis and long axis images using a semi-automated process.

2.1.5 | ^{31}P Phosphorus magnetic resonance spectroscopy

All ^{31}P -MRS was performed at 3T (Siemens Tim Trio MR system, Erlangen, Germany). Subjects lay prone with the

left ventricle centered over a modified dual-tuned heart/liver $^{31}\text{P}/^1\text{H}$ surface transmit/surface receive loop/butterfly coil with spectroscopy performed as previously described.¹⁷ A 3D acquisition-weighted chemical shift imaging (CSI) technique (TE = 0.3 ms) was used, in conjunction with an optimized radiofrequency pulse centered between the phosphocreatine and ATP resonances to maximize the signal to noise ratio, improve baseline artifacts and ensure uniform excitation of all spectral peaks. The acquisition matrix size was $16 \text{ mm} \times 8 \text{ mm} \times 8 \text{ mm}$, and the field of view was $240 \text{ mm} \times 240 \text{ mm} \times 200 \text{ mm}$, with 12 averages at the center of k-space. The Nuclear Overhauser Effect was used to increase the ^{31}P signal-to-noise ratio via proton radiofrequency irradiation.¹⁸ Proton localization images were used to obtain short axis left ventricular planes. To minimize potential signal contamination, two saturation bands were placed over the anterior chest-wall skeletal muscle and over the liver, respectively. During analysis, all spectra were coded to exclude descriptive data, with voxels selected independently, and analyzed blind using in-house custom software which implemented the AMARES algorithm for spectral quantification through the OXSA toolkit in Matlab.¹⁹ The quality of the spectral fit was assessed using the expected coefficient of variation in the measured PCr/ATP value based on the Cramer-Rao lower bounds. Spectra were determined to be of sufficient quality if they had a coefficient of variation below 20%. Of the nine data sets recorded, two were discarded due to poor spectral quality.

2.2 | Animal study methods

All animal experiments were performed in accordance with relevant legislation with personal, project, and institutional licenses granted under the UK Animals (Scientific Procedures) Act 1986. Age and weight-matched male Wistar rats in four separate cohorts were used, with eight animals in each cohort.

A dose of 50 mg/kg body weight of Acipimox was chosen based on work by other groups²⁰ and we performed pilot experiments to show this had peak effect in suppressing fatty acid levels over the first 1 to 2 hours post injection (see Supporting Data 1).

The study procedure is summarized in Figure 1. The first cohort (Unfed Acipimox) were briefly starved overnight and received an intraperitoneal (IP) injection of 2 μ L/g body weight of a solution containing 25 mg of Acipimox (Sigma Aldrich, Dorset, UK) in 1 mL of sterile saline (50 mg/kg body weight of the animal). The second cohort (Unfed Saline) were briefly starved overnight and received an intraperitoneal injection of 2 μ L/g body weight sterile saline. The cohorts were mixed by an investigator separate to the experiment allocating the solutions for injection in a random fashion, so the investigators handling the animals and subsequently analyzing the data were blinded to which received saline and which Acipimox. A third cohort (Fed Acipimox) was allowed to feed ad libitum on normal rodent chow (60% carbohydrate) and injected with 2 μ L/g body weight of the Acipimox solution (50 mg/kg) and a fourth cohort (Fed) were allowed to feed on chow ad libitum and did not receive an injection (Figure 1).

2.2.1 | Blood sampling

Venous blood samples were taken immediately prior to IP injection from the saphenous vein using Li-heparin-coated collection tubes, and then, again 1 hour after the injection. Blood samples were centrifuged at 300xg and 4°C and plasma transferred into separate tubes and stored at -80°C until further use. Glucose was analyzed with a point-of-care device (Accu-Check) in fresh whole blood, free fatty acids, β -hydroxybutyrate, tri-acylglycerol, and lactate were analyzed in plasma samples with a spectrophotometric assay (Randox, Crumlin, UK) and insulin with an ELISA kit (Mercodia, Uppsala, Sweden).

2.2.2 | MRI/MRS

One-hour postinjection, rats were anesthetized with 2% of isoflurane and loaded into a horizontal bore 7T spectrometer (VARIAN) in a custom-made cradle. ECG monitoring was undertaken throughout. A cine-FLASH sequence was used to assess cardiac function and volumes using a dual-tuned $^1\text{H}/^{13}\text{C}$ -volume coil and a four-channel ^1H -receive surface coil (Rapid Biomedical; FOV 51.2 mm² \times 51.2 mm², 1.6 mm axial slices, 128x128x8 matrix size, flip angle 15°, 4 averages). Hyperpolarized [$1\text{-}^{13}\text{C}$]pyruvate MRS was used to assess cardiac pyruvate dehydrogenase (PDH) flux, as described previously.²¹ Briefly, 1 mL of 80 mM hyperpolarized [$1\text{-}^{13}\text{C}$]pyruvate was injected into a tail vein over 10 seconds

through a pre-implanted cannula. A slice-selective MR spectrum (10 mm slab) was acquired from the cardiac region (60 acquisitions, 1 second TR, 15° Gaussian excitation pulse, 14 kHz bandwidth) using a two-element ^{13}C surface receive array coil (Rapid Biomedical) and volume ^{13}C excitation. Multi-coil data were either reconstructed via the whitened singular value decomposition method,²² or were elementwise manually phased to the pyruvate peak and added in phase. The first 30 seconds of spectra following the first appearance of the pyruvate peak were summed and quantified using AMARES/jMRUI as previously described.²³

2.2.3 | Euthanasia

At the end of the MRI/MRS experiment, the rats were terminally anesthetized with 5% of isoflurane in oxygen. Upon confirmation of deep anesthesia (loss of the corneal reflex), euthanasia was performed by rapid excision of the heart.

2.3 | Statistical analysis

Statistical analysis was performed using GraphPad Prism (GraphPad software, USA). All data were subjected to Kolmogorov-Smirnov tests to establish normal distribution and are presented as mean \pm standard deviation. Paired equal variance Student's *t* tests were performed for pre and post intervention data sets in humans or animals. One-way ANOVA was used when analyzing the multiple animal data sets with a post hoc Bonferroni test for multiple comparisons. Correlations, where relevant, were assessed with Pearson's correlation analysis. A probability of $P < .05$ was considered significant.

3 | Results

3.1 | Results: Human studies

3.1.1 | Baseline characteristics

All nine participants (average age 24 ± 3 y, male $n = 6$) were normotensive, normocholesterolemic, and normoglycemic at the time of the study. Baseline characteristics are shown in Table 1.

3.1.2 | Circulating metabolites and hemodynamic profile

Four hours after nicotinic acid ingestion, circulating levels of FFAs fell (from baseline 0.19 ± 0.07 mmol/L to 0.03 ± 0.04 mmol/L, $P < .001$), Figure 2 and table 2.

Circulating glucose levels, insulin, and β -hydroxybutyrate levels were not statistically different (all $P > .05$). There were no changes in systolic blood pressure, diastolic blood pressure, or heart rate.

TABLE 1 Baseline characteristics for human participants (n = 9)

Patient characteristics	
Anthropometrics	
Age (y)	24 \pm 3
Height (m)	1.71 \pm 0.1
Body mass index (kg/m ²)	24.1 \pm 2.0
Weight (kg)	71 \pm 11
Systolic blood pressure (mmHg)	119 \pm 10
Diastolic blood pressure (mmHg)	74 \pm 8
Pulse pressure (mmHg)	45 \pm 9
Circulating metabolites	
Fasting glucose (mmol/L)	4.5 \pm 0.9
Fasting cholesterol (mmol/L)	4.3 \pm 0.7

3.1.3 | Myocardial energetics and left ventricular function

Nicotinic acid caused a significant decrease in systolic function (absolute reduction 3.4%, LVEF baseline 64 \pm 8% to 60 \pm 7%, $P = .027$), Figure 2 and table 2. In line with this, peak circumferential systolic strain increased (from -20.3 ± 4.1 to -18.2 ± 4 , $P = .005$), although radial strain did not significantly change. There was a fall in myocardial PCr/ATP ratio (baseline 2.16 \pm 0.40 to 1.78 \pm 0.14, $P = .037$).

3.1.4 | Correlations between circulating glucose and myocardial function

Pooling the baseline and 4-hour data, glucose levels correlated with cardiac function by global radial strain ($R = 0.55$, $P = .018$), global longitudinal strain ($R = 0.548$, $P = .018$), and ejection fraction ($R = 0.613$, $P = .007$, Figure 3). No other significant correlations were observed.

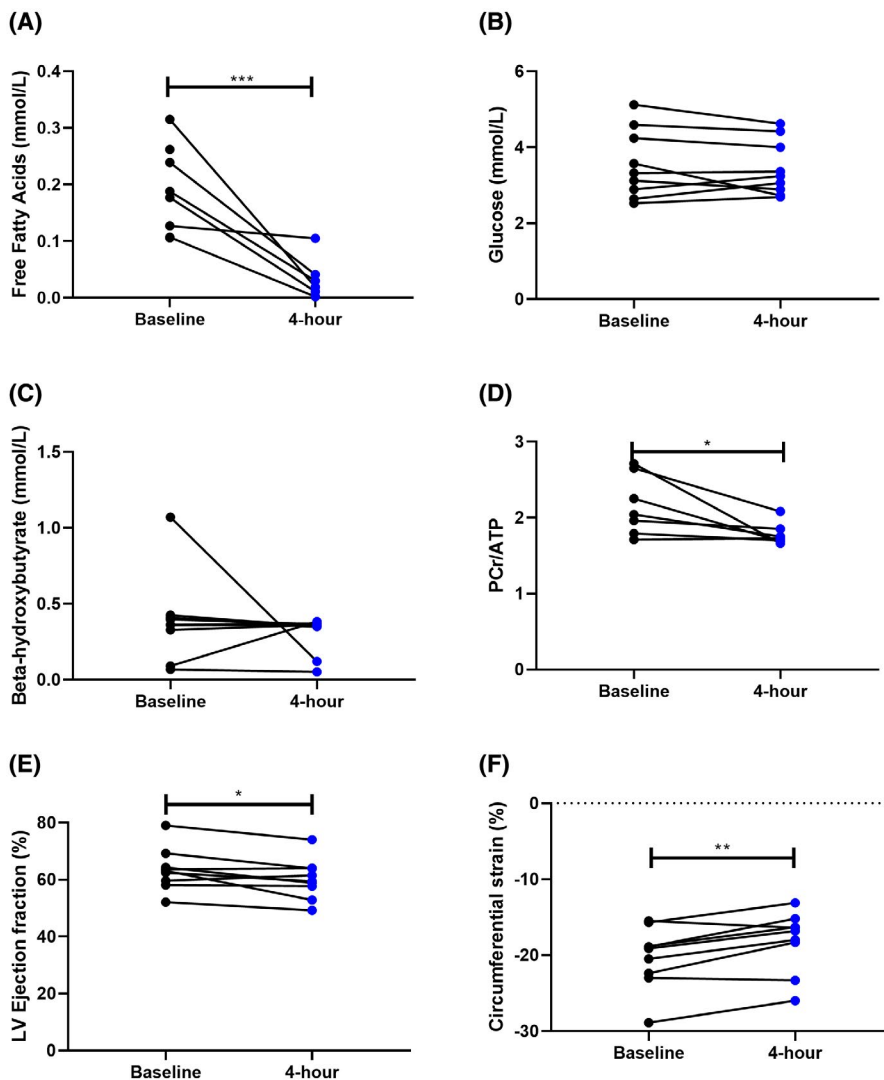
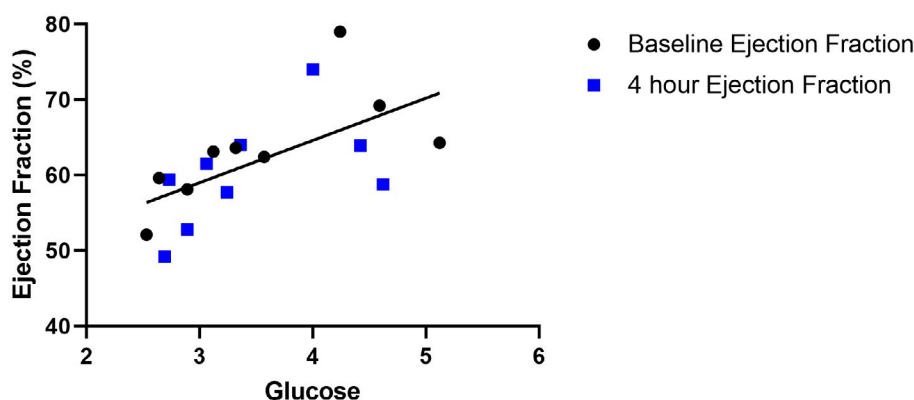


FIGURE 2 Data from human nicotinic acid studies. Nine sets of data. Panel A, serum free fatty acids (mmol/L) prior to (baseline) and 4 hours following the administration of oral nicotinic acid. Panel B, serum glucose prior to (baseline) and 4 hours following the administration of oral nicotinic acid. Panel C, Serum Beta-hydroxybutyrate prior to (baseline) and 4 hours following the administration of oral nicotinic acid. Panel D, Phosphocreatine/ATP ratio by magnetic resonance spectroscopy prior to (baseline) and 4 hours following the administration of oral nicotinic acid. Panel E, left ventricular ejection fraction calculated from a cardiovascular magnetic resonance left ventricular short axis stack prior to (baseline) and 4 hours following the administration of oral nicotinic acid. * $P < .05$, ** $P < .01$, *** $P < .001$ by paired t-test. Panel F, global circumferential strain calculated from magnetic resonance imaging prior to (baseline) and 4 hours following the administration of oral nicotinic acid

TABLE 2 Human data from nicotinic acid study

	Nicotinic acid infusion		
	Baseline	4 h	<i>P</i> value
Circulating metabolites			
Fatty acids (mmol/L)	0.19 ± 0.07	0.03 ± 0.04	<.001
Ketone (mmol/L)	0.39 ± 0.07	0.29 ± 0.03	.41
Glucose (mmol/L)	3.56 ± 0.91	3.44 ± 0.73	.78
Insulin (mU/L)	0.21 ± 0.02	0.17 ± 0.05	.15
Hemodynamics			
Systolic blood pressure (mmHg)	115 ± 12	108 ± 10	.08
Diastolic blood pressure (mmHg)	62 ± 8	64 ± 5	.65
Heart rate (beats per minute)	59 ± 9	57 ± 8	.77
Myocardial energetics			
Myocardial PCr/ATP	2.16 ± 0.40	1.78 ± 0.14	.037
Left ventricular systolic function			
LVEF (%)	63.5 ± 7.5	60.1 ± 7.1	.03
Circumferential Strain (%)	-20.3 ± 4.1	-18.2 ± 4.0	.005
Radial Strain (%)	40.3 ± 16.1	35.9 ± 15.0	.24

Note: n = 9, excepting for PCr/ATP data where two data sets were excluded owing to low data quality. Bold values are significant at the <.05 level.

**FIGURE 3** Correlation between serum glucose (mmol/L) and cardiac ejection fraction as assessed by cardiac MRI short axis stack. Data are pooled from the baseline (predrug) and 4-hour time points from nine individuals to create 18 data points

4 | Results: Animal studies

There were small but statistically significant weight differences between unfed and fed groups (average unfed 262 ± 10 g vs average fed 288 ± 13 g, $P < .0001$, table in data supplement), which was likely due to the overnight starvation: rats consume approximately 15–30 g food per day (and most of this through the night).

4.1 | Circulating metabolites

Acipimox caused a fall in FFAs in the unfed animals, but no change in the fed animals, nor was there a change in the

animals given saline. As expected, unfed animals given Acipimox had significantly lower FFA ($P < .001$) than those given saline, see Figure 4A and Table 3.

Beta-hydroxybutyrate was seen to rise only in the unfed animals injected with saline (from 0.65 ± 0.18 mmol/L to 1.17 ± 0.45 mmol/L, $P = .019$), while there was no significant change in unfed animals injected with Acipimox. In the fed animals, levels were low throughout.

Blood glucose was higher in fed than unfed animals and there was a statistically significant increase in blood glucose in the unfed animals injected with Acipimox (from 5.4 ± 0.8 to 6.4 ± 1.1 , $P = .018$), which was not seen in the saline injected animals, nor the fed animals injected with Acipimox. Insulin levels were generally below the lower limit

of assay detection in unfed animals. In fed animals, Acipimox caused circulating insulin to fall from 1695 ± 891 ng/L to 550 ± 222 ng/L ($P = .005$); leaving these fed animals given Acipimox with significantly lower insulin levels than those fed animals not injected with Acipimox (fed insulin level prior to scan 1181 ± 432 ng/L, $P = .002$ compared to unfed level prior to scan). FFAs inversely correlated with whole blood glucose ($R = 0.53$, $P = .003$) and positively correlated with plasma β -hydroxybutyrate ($R = 0.77$, $P < .001$).

4.2 | Contractility

In both fed and unfed animals, those given Acipimox had lower cardiac contractility compared to their respective controls (Table 4 and Figure 5). In a similar pattern to that seen in humans, unfed animals had lower LVEF (absolute reduction 8%, saline $68 \pm 4\%$ vs Acipimox $60 \pm 3\%$ $P = .03$) and also lower cardiac output indexed to body mass ($368 \pm 35 \times 10^{-3}$ mL/min/g vs $426 \pm 53 \times 10^{-3}$ mL/min/g, $P = .02$). In fed animals, the ejection fractions were not significantly changed by Acipimox, however, there was a difference in cardiac output indexed to body mass ($395 \pm 50 \times 10^{-3}$ mL/min/g vs $471 \pm 45 \times 10^{-3}$ mL/min/g, $P = .014$). There were no significant differences between the two groups which had not received Acipimox.

4.3 | Hyperpolarized [$1\text{-}^{13}\text{C}$]pyruvate MRS

Values for the hyperpolarized data are summarized in Table 4 and Figure 6 and are given as summed spectra acquired every second over 30 seconds from the first appearance of the pyruvate peak, indexed to pyruvate peak height over the same time. Values are expressed as a ratio of signal intensity.

Unfed animals injected with Acipimox had higher pyruvate dehydrogenase (PDH) flux (defined as the ratio of bicarbonate:pyruvate) than those given the saline control ($P = .0019$). However, while elevated, bicarbonate production after

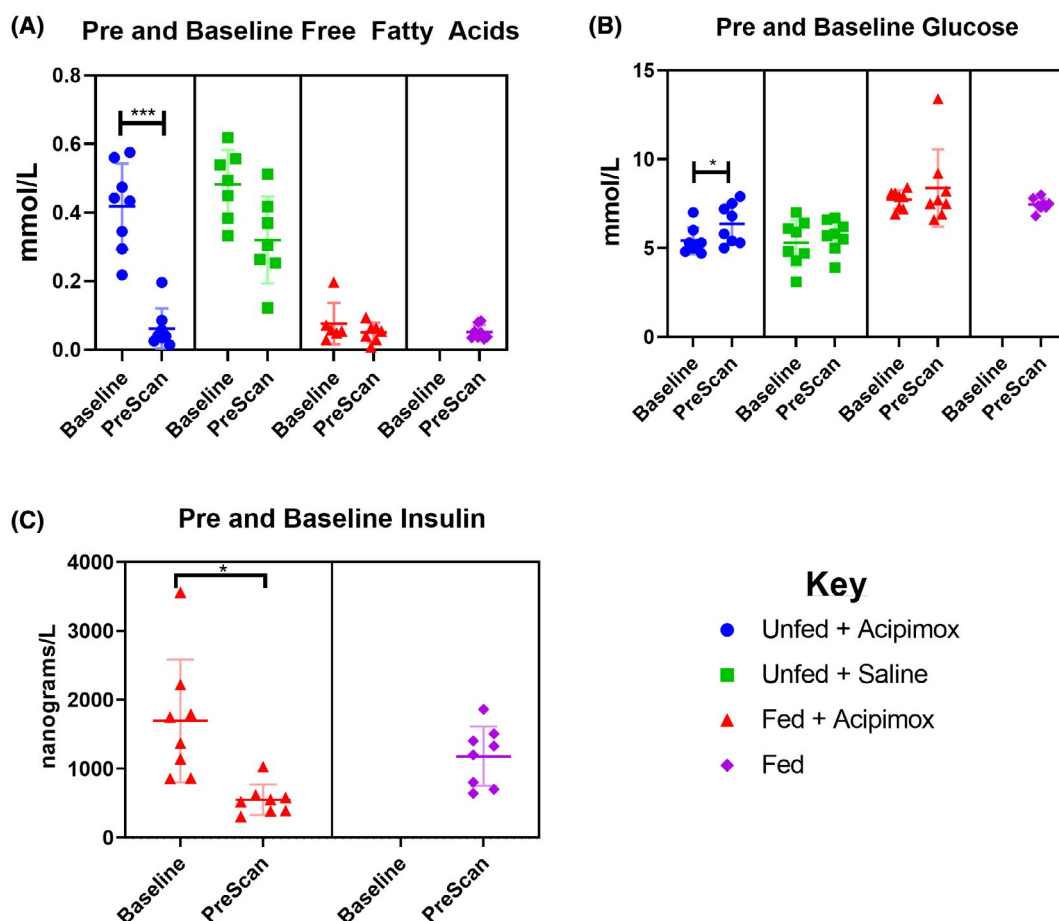


FIGURE 4 Metabolite rat data. * $P < .05$, ** $P < .01$, *** $P < .001$ by paired t-test. Panel A, Serum free fatty acid (mmol/L) at baseline (prior to any drug administration) and immediately prior to scan (1 hour following drug administration). $n = 8$ per group. Panel B, Serum glucose (mmol/L) at baseline (prior to any drug administration) and immediately prior to scan (1 hour following drug administration). $n = 8$ per group. Panel C, Serum insulin (ng/L) at baseline (prior to any drug administration) and immediately prior to scan (1 hour following drug administration). $n = 8$ per group

TABLE 3 Circulating metabolites for the animal studies

Circulating metabolite	Unfed + Saline		Unfed + Acipimox		Fed		Fed + Acipimox		Group ANOVA	
	Pre	Post	Pre	Post	Post	Post	Pre	Post	Pre	Post
Glucose (mmol/L)	5.3 ± 1.3	5.7 ± 0.9	5.4 ± 0.8	6.4 ± 1.1*	7.5 ± 0.4	7.5 ± 0.4	7.7 ± 0.5	8.4 ± 2.1	<0.001	0.002
Free fatty acids (mmol/L)	0.48 ± 0.1	0.32 ± 0.12	0.42 ± 0.13	0.06 ± 0.06*	0.05 ± 0.02	0.05 ± 0.02	0.07 ± 0.06	0.06 ± 0.02	<0.001	<0.001
Beta-hydroxybutyrate (mmol/L)	0.65 ± 0.18	1.17 ± 0.45*	0.46 ± 0.19	0.38 ± 0.31	0.03 ± 0.01	0.03 ± 0.01	0.05 ± 0.05	0.04 ± 0.03	<0.001	<0.001
Tri-acyl glycerol (mmol/L)	0.67 ± 0.56	0.83 ± 0.45	0.61 ± 0.41	0.39 ± 0.35*	0.83 ± 0.55	0.83 ± 0.55	0.65 ± 0.88	0.38 ± 0.47	0.78	0.12
Lactate (mmol/L)	0.85 ± 0.41	1.02 ± 0.31	1.13 ± 0.16	1.21 ± 0.35	1.32 ± 0.75	1.32 ± 0.75	0.87 ± 0.98	0.55 ± 0.6	0.59	0.06
Insulin (ng/L)	BLD	BLD	BLD	BLD	1181 ± 432	1181 ± 432	1695 ± 891	550 ± 222*	-	-

Abbreviation: BLD, below lower limit of assay detection.
**P* < .05 for the baseline vs postinjection comparison via paired two-way t test analysis.

Acipimox was 66% of that observed in fed animals (*P* = .02). PDH flux in fed rats given Acipimox was also lower than that observed in fed animals without Acipimox (*P* = .04). Unfed animals had a higher lactate:pyruvate ratio than fed animals (0.18 ± 0.06 vs 0.11 ± 0.04 , *P* < .001), while Acipimox administration did not significantly alter lactate metabolism. There were no significant changes in alanine production.

Across all groups, free fatty acids inversely correlated with bicarbonate production (*R* = 0.64, *P* < .001), suggesting an increase in glucose oxidation as FFA availability declined. In the unfed animals, bicarbonate production was negatively correlated with cardiac index (*R* = 0.73, *P* = .001), but there was no such correlation in fed animals. In the unfed animals, blood glucose correlated with bicarbonate production (*R* = 0.57, *P* = .021) but there was no correlation in the fed group. These correlations are demonstrated in Figure 7.

In summary, in the unfed animals, Acipimox increased bicarbonate production (indicating an increase in PDH flux), although not to the levels seen in animals allowed to feed ad libitum. In the fed animal, it had the opposite effect, reducing PDH flux. As there was no alteration in lactate production to indicate increased glycolysis, this would suggest a submaximal rise in glucose uptake limited glucose oxidation in the unfed rat, and a fall in glucose uptake and oxidation in the fed rat.

5 | DISCUSSION

Here, we show that following nicotinic acid receptor agonist administration in fasting humans, there is a depression of contractile function and a decrease in the cardiac PCr/ATP ratio. In rats, the reduction in LV function following nicotinic acid receptor agonist administration was linked to a reduction in fatty acid availability and/or myocardial glucose oxidation.

5.1 | Effects of lowering fatty acid supply to the human heart in fasting participants

We showed here that, when fatty acid supply was lowered with a nicotinic acid receptor agonist in humans who had been requested to fast, an 18% reduction of PCr/ATP occurred (showing the available energy for contraction was reduced), which was associated with a decline in systolic function. Given what we know about cardiac metabolic flexibility, a reduction in FFA utilization should simply result in increased glucose uptake and metabolism via Randle cycle mechanisms⁸ to offset the decrease in FFA availability. Indeed, in PET studies on fasting volunteers, myocardial glucose uptake with nicotinic acid administration increases to a

TABLE 4 Animal contractility data and hyperpolarized [$1\text{-}^{13}\text{C}$]pyruvate MRS

	Unfed + Saline	Unfed + Acipimox	Fed	Fed + Acipimox	Group comparison ANOVA <i>P</i> value
LVEF (%)	67.8 ± 3.6*	60 ± 3.1**	70.4 ± 3.5***	67.5 ± 8.9	.004
CO (mL/min)	111 ± 15.8***	97.2 ± 12.3	135 ± 13***	115 ± 18.4	<.001
CO index (mL/min/g)	426 ± 53	368 ± 35	471 ± 45***	395 ± 50***	.001
Cardiac metabolism					
PDH (Bicarbonate, $\times 10^{-4}$)	182 ± 114* ^{###}	486 ± 139	726 ± 201***	512 ± 130 ^{#,###}	<.001
LDH (Lactate, $\times 10^{-4}$)	1220 ± 243 ^{###}	993 ± 425	1970 ± 613***	1620 ± 508	.001
ALAT (Alanine, $\times 10^{-4}$)	185 ± 159	145 ± 149	250 ± 97	176 ± 123	.47

Abbreviations: ALAT, alanine transaminase flux expressed as alanine production: alanine peak height indexed to pyruvate peak height. LDH, lactate dehydrogenase flux expressed as lactate production: lactate peak height indexed to pyruvate peak height. PDH, pyruvate dehydrogenase flux expressed as bicarbonate production: bicarbonate peak height indexed to pyruvate peak height.

MRS values are shown as summed peak height over 30 s indexed to summed pyruvate peak height over same time. Group comparisons are given by one-way ANOVA. The following symbols denote *P* value < 0.05 for;

*Unfed + Acipimox vs Unfed + Saline.

**Unfed + Acipimox vs Fed + Acipimox.

***Unfed + Acipimox vs Fed.

[#]Unfed + Saline vs Fed + Acipimox.

^{###}Unfed + Saline vs Fed.

^{####}Fed vs Fed + Acipimox.

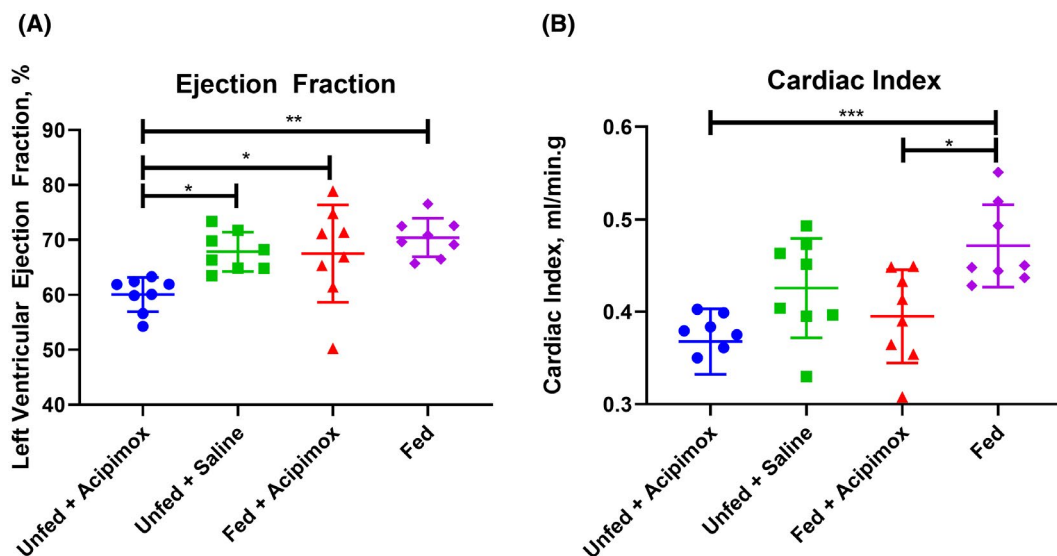


FIGURE 5 MRI rat data showing cardiac contractility. * *P* < .05, ** *P* < .01, *** *P* < .001 by post hoc Bonferroni test. Panel A, Cardiac ejection fraction derived from left ventricular short axis stack by group. *n* = 8 per group. Panel B, Cardiac output derived from left ventricular stroke volume (from short axis stack) multiplied by heart rate indexed to body weight by group. *n* = 8 per group

level comparable to insulin-glucose clamp,²⁴ and it has previously been suggested that the increase in glucose metabolism from FFA metabolism inhibition would be sufficient to offset a loss of FFA availability.²⁵ However, PET only shows glucose uptake rather than metabolism, hence, we used [$1\text{-}^{13}\text{C}$]pyruvate MRS to determine changes in glucose metabolism in the rat heart to further explain our observations in human volunteers.

5.2 | [$1\text{-}^{13}\text{C}$]pyruvate magnetic resonance spectroscopy and cardiac function in healthy rats

We used hyperpolarized [$1\text{-}^{13}\text{C}$]pyruvate MRS to define the metabolic fate of pyruvate, and hence, discriminate glucose oxidation from glucose uptake.²⁶ In discussion of the results, we focus on two competing mechanisms. The first are the concentrations of blood glucose and plasma insulin, which will act

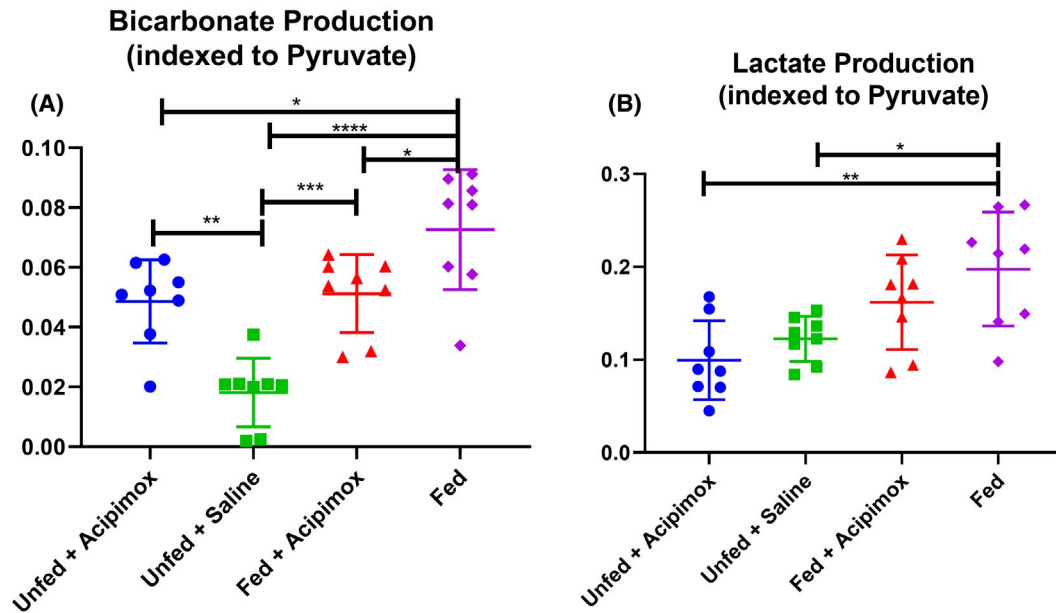


FIGURE 6 Rat Magnetic Resonance Spectroscopy rat data. * $P < .05$, ** $P < .01$, *** $P < .001$, **** $P < .0001$ by post hoc Bonferroni test. Panel A, Bicarbonate peak height over 30 s indexed to pyruvate peak height over 30 s by $[1-^{13}\text{C}]$ pyruvate magnetic resonance spectroscopy between different groups. $n = 8$ per group. Panel B, Lactate peak height over 30 s indexed to pyruvate peak height over 30 s by $[1-^{13}\text{C}]$ pyruvate magnetic resonance spectroscopy between different groups. $n = 8$ per group

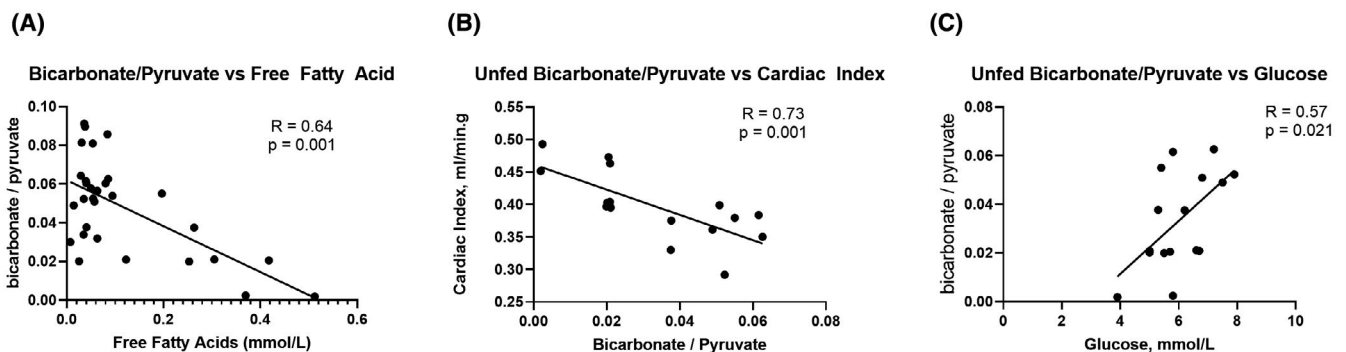


FIGURE 7 Correlations seen in rat data. Panel A, Bicarbonate peak height over 30 s indexed to pyruvate peak height over 30 s by $[1-^{13}\text{C}]$ pyruvate magnetic resonance spectroscopy compared to serum free fatty acids (postinjection or immediately prior to scanning). Panel B, Cardiac index compared to bicarbonate peak height over 30 s indexed to pyruvate peak height over 30 s by $[1-^{13}\text{C}]$ pyruvate magnetic resonance spectroscopy in unfed animals. Panel C, Bicarbonate peak height over 30 s indexed to pyruvate peak height over 30 s by $[1-^{13}\text{C}]$ pyruvate magnetic resonance spectroscopy compared to serum glucose (postinjection or immediately prior to scanning) in unfed animals

to increase glucose uptake and elevate pyruvate dehydrogenase flux, increasing glucose metabolism. The second is the plasma concentration of free fatty acids: the metabolism of which will inhibit glucose metabolism through Randle cycle actions to activate glucose uptake, phosphofructokinase, and pyruvate dehydrogenase, decreasing pyruvate dehydrogenase flux.

5.2.1 | $[1-^{13}\text{C}]$ pyruvate magnetic resonance spectroscopy in healthy fed rats

These animals show a large bicarbonate/pyruvate ratio consistent with high pyruvate dehydrogenase flux. This would be consistent with high levels of blood glucose and high levels

of insulin driving glucose uptake and metabolism, and would be expected given the carbohydrate rich nature of the chow. In addition, low levels of circulating FFAs would also result in a low level of myocardial fatty acid metabolism, and hence, minimal inhibition of pyruvate dehydrogenase, maximizing glucose metabolism.

5.2.2 | $[1-^{13}\text{C}]$ pyruvate magnetic resonance spectroscopy in healthy unfed rats given saline placebo

In these animals which were starved overnight, the bicarbonate/pyruvate ratio is low, demonstrating low pyruvate

dehydrogenase flux. This would also be expected given that blood glucose and plasma insulin were low and FFA levels high. As such FFA metabolism will dominate in the unfed state, causing maximal inhibition of pyruvate dehydrogenase while glucose supply would also be low.

Lactate/pyruvate ratio was lower in unfed animals compared to fed animals, additionally demonstrating low lactate dehydrogenase exchange, again expected given the low glucose supply.

5.2.3 | [1-¹³C]pyruvate magnetic resonance spectroscopy in healthy unfed rats given the nicotinic acid receptor agonist Acipimox

These animals exhibited higher pyruvate dehydrogenase flux than unfed animals given the saline placebo, but lower than that seen in the fed rats. Here, as FFA levels were suppressed to levels comparable to the fed state, it would be expected that FFA-mediated inhibition of pyruvate dehydrogenase via the Randle cycle would be minimized, and pyruvate dehydrogenase flux elevated. However, we propose that although there was a small rise in blood glucose, as plasma insulin levels remained low, glucose entry into the glycolytic pathway would not be increased and this may account for the reduced pyruvate dehydrogenase flux compared to fed rats.

5.2.4 | [1-¹³C]pyruvate magnetic resonance spectroscopy in healthy fed rats given the nicotinic acid receptor agonist Acipimox

Compared to the fed animals not given Acipimox, the pyruvate dehydrogenase flux in fed animals given Acipimox was lower; in fact it was not significantly different from unfed animals given Acipimox. As FFA levels were low, Randle cycle-mediated pyruvate dehydrogenase inhibition should be minimal in this group. However, while serum glucose was comparable to that seen in the fed animals not given Acipimox, insulin levels were lower. We therefore hypothesize that the lower pyruvate dehydrogenase flux in this group was caused by a lower glucose supply to glycolysis, mediated by reduced insulin levels, which would have a direct effect to cause a fall in myocardial glucose uptake. The trend toward a fall in lactate:pyruvate ratio (LDH exchange) would be supportive of this. While we were unable to detect a drop in insulin levels in human participants given nicotinic acid, this has been observed in other studies.^{12,13}

5.2.5 | Cardiac contractility in healthy rats

As in the fasting humans, Acipimox treatment depressed ejection fraction in the unfed rats. In line with this, in the

fed rats, a significant lower cardiac output indexed to body weight was observed after Acipimox injection. Interestingly, there was a negative correlation between cardiac index and pyruvate dehydrogenase flux in all of the unfed animals, possibly an indirect effect, as the animals with the greatest fall in FFAs had the largest rise in pyruvate dehydrogenase flux.

5.2.6 | Circulating ketone levels in healthy rats

A small rise in circulating β -hydroxybutyrate was seen in the unfed animals injected with saline which was not seen in the animals injected with Acipimox. While we did not specifically investigate ketone metabolism in this study, impaired ketone production secondary to a fall in lipolysis may further impair myocardial energy metabolism.

5.3 | Potential mechanisms of nicotinic acid-induced ventricular impairment

Nicotinic acid, and its Acipimox derivative, act on the GPR109a receptor in adipose tissue to inhibit lipolysis.⁶ GPR109a is also expressed in pancreatic beta cells: here, its activation reduces glucose-stimulated insulin secretion via PPAR- γ and cAMP,^{27,28} with the fall in insulin in turn reducing cellular glucose uptake and metabolism in target tissues such as the heart. This gives rise to the clinical observation that nicotinic acid receptor agonism impairs glucose tolerance and elevates serum glucose levels.²⁹ The myocardium expresses GLUT-1 transporters, which are insulin-insensitive and GLUT-4 transporters, which are insulin sensitive. The GLUT-1 transporter's rate is influenced by glucose concentration (although practically mM is sufficiently low that it is almost always operating at Vmax), while GLUT-4 requires insulin to fulfil its role.³⁰ Insulin also has effects to increase activity of enzymes involved in glycolysis such as phosphofructokinase² and pyruvate dehydrogenase itself, via pyruvate dehydrogenase kinase.³¹ It therefore follows that glucose can be taken up and metabolized by the heart in conditions of low insulin, but maximizing glucose utilization requires additional insulin.

In fed animals, although Acipimox does not significantly change the concentrations of blood glucose, insulin concentrations fall and we see lower pyruvate dehydrogenase flux. This is predictable from the known actions of insulin on GLUT-4, glycolytic pathways, and pyruvate dehydrogenase. There are subtle indications of an impairment of function associated with this as the cardiac output indexed to body weight is lower than in the fed animals not given Acipimox.

In the unfed state, levels of circulating free fatty acids are (as expected) higher than in the fed state with pyruvate

dehydrogenase flux lower as the heart shifts toward higher levels of fatty acid metabolism in the absence of glucose and insulin. Here, the effects of Acipimox are more difficult to understand but nonetheless present. We would expect that the rise in blood glucose following Acipimox injection would result in a rise in insulin secretion, however, levels of insulin remain below the lower limit of detection. Given circulating FFA levels (and, it would follow, fat metabolism) postinjection are similar to those seen in fed animals, we would expect pyruvate dehydrogenase flux to be similar, yet it is lower. An explanation linking these observations is that, while there was an increase in blood glucose to offset the fall in free fatty acids, the effect of Acipimox was likely to reduce glucose-stimulated insulin secretion, which ultimately prevents pyruvate dehydrogenase flux from reaching the levels seen in the fed rats whose insulin secretion matches the serum glucose levels. This explains how the unfed animals given Acipimox have the lowest left ventricular ejection fraction seen in all the groups.

A lack of insulin causing submaximal glucose oxidation in both unfed and fed states would explain the functional deficiencies observed: acetyl-CoA entry into the TCA cycle would be reduced from both glucose and fatty acid routes, effectively starving the heart of substrate to produce ATP. The fall in PCr/ATP seen in the human participants would then reflect high energy phosphate supply from PCr acting as a buffer which is depleted as oxidative phosphorylation rate is outstripped by ATP demand.

As nicotinic acid acts as an NAD⁺ precursor, it has been suggested that it may boost mitochondrial NAD⁺, and therefore, oxidative capacity, which has been demonstrated in human skeletal muscle cells.³² While redox state was not formally tested in these animals, we are able to make some assumptions based on the [1-¹³C]lactate: [1-¹³C]pyruvate ratio. This reaction is closely coupled to NAD⁺ and our group has previously shown the ratio to be inversely proportional to the NAD⁺/NADH ratio³³ so it can be used to noninvasively assess redox state. In both groups, there was a trend toward a reduction in [1-¹³C]lactate: [1-¹³C]pyruvate ratio with Acipimox administration (suggesting a rise in NAD⁺/NADH ratio), however, this did not reach statistical significance. Therefore, we are unable to account for alterations in cardiac performance stemming from changes in redox state alone. Lactate:pyruvate ratio from hyperpolarized [1-¹³C] pyruvate was lower in unfed animals compared to their fed counterparts, although interestingly this is the opposite trend to that seen in the liver,³⁴ presumably reflecting the different LDH isoforms.

5.4 | Comparison with other studies

The increase in glucose uptake in the unfed state is consistent with FDG-PET studies, which have demonstrated that the

rise in myocardial glucose uptake accompanying nicotinic acid receptor agonism was insufficient to offset the decline in FFA uptake, with myocardial oxygen consumption falling and the decline in LV function being proportional to the drop in FFA uptake.¹⁴ Where LV function was compared between MRI and PET in a protocol involving Acipimox administration in the PET group only, not only was LV function consistently lower in the PET arm of the study, but also more dysfunctional myocardial segments were seen on PET.³⁵ It may be that the administration of a nicotinic acid receptor agonist in the PET arm resulted in lower insulin levels, impaired cardiac metabolism, and a greater degree of dysfunction in ischemic myocardium.

6 | LIMITATIONS

In the human arm of the study, we are limited by the lack of ¹³C MR spectroscopy to demonstrate the fate of pyruvate. In the animal arm of the study, we are limited by the lack of a saline placebo in the fed arm of the study and it may be questioned whether a stress response to IP injection alters the metabolic substrate selection in the heart. In both studies, we cannot demonstrate the fates of other metabolites such as free fatty acids or ketones, only infer them from circulating concentrations. The study duration for humans was 4 hours and for animals this was 1 hour; in addition, the entire human cohort was fasting while half of the rat cohort were unfed, hence, these results may not represent the effect of chronic treatment in the fed state, which would be the state of patients.

7 | CONCLUSIONS

We have shown here that healthy heart function can be altered by limiting its supply of metabolic substrates, confirming the importance of myocardial substrate metabolism to cardiac contractile function. In particular, we have shown that by reducing circulating fatty acids and inhibiting glucose-stimulated insulin secretion, nicotinic acid receptor agonists starve the heart of metabolic substrate. While there was an increase in glucose metabolism in the unfed state, it appears to be insufficient to make up for the loss of fatty acids, and hence, cardiac function was compromised as a result. In the fed state, glucose metabolism falls.

Although an acute study, these observations shed light on why nicotinic acid receptor agonists, such as Acipimox, have failed to bring about benefits for patients with heart failure. The use of nicotinic acid receptor agonists in PET protocols to stimulate glucose uptake may give rise to falsely low readings of left ventricular function.

ACKNOWLEDGMENTS

JJM would like to acknowledge an EPSRC Doctoral Prize Fellowship (ref. EP/M508111/1) and Novo Nordisk Postdoctoral Research Fellowship run in conjunction with the University of Oxford.

CONFLICT OF INTEREST

None to declare.

AUTHOR CONTRIBUTIONS

S Neubauer, K Clarke, D Tyler, and O Rider conceived the research. O Rider and Y Emmanuel performed the human experiments. Y Emmanuel, A Lewis, and W Watson analyzed the human data. K Timm and W Watson performed and analyzed data from the animal experiments. J Miller designed MRS sequences and analysis packages for ^{13}C data. W Watson and O Rider wrote the paper with input from the other authors.

REFERENCES

- Karwi QG, Uddin GM, Ho KL, Lopaschuk GD. Loss of metabolic flexibility in the failing heart. *Front Cardiovasc Med*. 2018;5:68.
- Stanley WC, Recchia FA, Lopaschuk GD. Myocardial substrate metabolism in the normal and failing heart. *Physiol Rev*. 2005;85:1093-1129.
- Veech RL. The therapeutic implications of ketone bodies: the effects of ketone bodies in pathological conditions: ketosis, ketogenic diet, redox states, insulin resistance, and mitochondrial metabolism. *Prostag Leukotr Ess*. 2004;70:309-319.
- Neubauer S. Mechanisms of disease—the failing heart—an engine out of fuel. *New Engl J Med*. 2007;356:1140-1151.
- Lopaschuk GD, Ussher JR, Folmes CDL, Jaswal JS, Stanley WC. Myocardial fatty acid metabolism in health and disease. *Physiol Rev*. 2010;90:207-258.
- Tunaru S, Kero J, Schaub A, et al. PUMA-G and HM74 are receptors for nicotinic acid and mediate its anti-lipolytic effect. *Nat Med*. 2003;9:352-355.
- Randle PJ, Garland PB, Hales CN, Newsholme EA. The glucose fatty-acid cycle. Its role in insulin sensitivity and the metabolic disturbances of diabetes mellitus. *Lancet*. 1963;1:785-789.
- Hue L, Taegtmeyer H. The Randle cycle revisited: a new head for an old hat. *Am J Physiol Endocrinol Metab*. 2009;297:E578-E591.
- Knuuti MJ, Yki-Jarvinen H, Voipio-Pulkki LM, et al. Enhancement of myocardial [fluorine-18]fluorodeoxyglucose uptake by a nicotinic acid derivative. *J Nucl Med*. 1994;35:989-998.
- Knuuti MJ, Maki M, Yki-Jarvinen H, et al. The effect of insulin and FFA on myocardial glucose uptake. *J Mol Cell Cardiol*. 1995;27:1359-1367.
- Halbirk M, Norrelund H, Moller N, et al. Suppression of circulating free fatty acids with acipimox in chronic heart failure patients changes whole body metabolism but does not affect cardiac function. *Am J Physiol Heart Circ Physiol*. 2010;299:H1220-H1225.
- Wolf P, Winhofer Y, Krssak M, et al. Suppression of plasma free fatty acids reduces myocardial lipid content and systolic function in type 2 diabetes. *Nutr Metab Cardiovasc Dis*. 2016;26:387-392.
- Lehto HR, Parkka J, Borra R, et al. Effects of acute and one-week fatty acid lowering on cardiac function and insulin sensitivity in relation with myocardial and muscle fat and adiponectin levels. *J Clin Endocrinol Metab*. 2012;97:3277-3284.
- Tuunanen H, Engblom E, Naum A, et al. Free fatty acid depletion acutely decreases cardiac work and efficiency in cardiomyopathic heart failure. *Circulation*. 2006;114:2130-2137.
- Rider OJ, Francis JM, Ali MK, et al. Determinants of left ventricular mass in obesity; a cardiovascular magnetic resonance study. *J Cardiovasc Magn Reson*. 2009;11:9.
- Rider OJ, Lewandowski A, Nethononda R, et al. Gender-specific differences in left ventricular remodelling in obesity: insights from cardiovascular magnetic resonance imaging. *Eur Heart J*. 2013;34:292-299.
- Tyler DJ, Emmanuel Y, Cochlin LE, et al. Reproducibility of ^{31}P cardiac magnetic resonance spectroscopy at 3 T. *NMR Biomed*. 2009;22:405-413.
- Li C, Negendank W, Murphy-Boesch J, MsK RN, Brown T. Molar quantitation of hepatic metabolites in vivo in proton-decoupled, nuclear overhauser effect enhanced ^{31}P NMR spectra localized by three-dimensional chemical shift imaging. *NMR Biomed*. 1996;9:141-155.
- Purvis LAB, Clarke WT, Biasioli L, Valkovic L, Robson MD, Rodgers CT. OXSA: An open-source magnetic resonance spectroscopy analysis toolbox in MATLAB. *PLoS One*. 2017;12:e0185356.
- Donati A, Cavallini G, Carresi C, Gori Z, Parentini I, Bergamini E. Anti-aging effects of anti-lipolytic drugs. *Exp Gerontol*. 2004;39:1061-1067.
- Le Page LM, Rider OJ, Lewis AJ, et al. Assessing the effect of hypoxia on cardiac metabolism using hyperpolarized (^{13}C) magnetic resonance spectroscopy. *NMR Biomed*. 2019;32:e4099.
- Rodgers CT, Robson MD. Receive array magnetic resonance spectroscopy: Whittened singular value decomposition (WSVD) gives optimal Bayesian solution. *Magn Reson Med*. 2010;63:881-891.
- Le Page LM, Rider OJ, Lewis AJ, et al. Increasing pyruvate dehydrogenase flux as a treatment for diabetic cardiomyopathy: a combined ^{13}C hyperpolarized magnetic resonance and echocardiography study. *Diabetes*. 2015;64:2735-2743.
- Stone CK, Holden JE, Stanley W, Perlman SB. Effect of nicotinic acid on exogenous myocardial glucose utilization. *J Nucl Med*. 1995;36:996-1002.
- Opie LH, Knuuti J. The adrenergic-fatty acid load in heart failure. *J Am Coll Cardiol*. 2009;54:1637-1646.
- Schroeder MA, Cochlin LE, Heather LC, Clarke K, Radda GK, Tyler DJ. In vivo assessment of pyruvate dehydrogenase flux in the heart using hyperpolarized carbon-13 magnetic resonance. *Proc Natl Acad Sci USA*. 2008;105:12051-12056.
- Chen L, So WY, Li SYT, Cheng Q, Boucher BJ, Leung PS. Niacin-induced hyperglycemia is partially mediated via nicotinic receptor GPR109a in pancreatic islets. *Mol Cell Endocrinol*. 2015;404:56-66.
- Wang N, Guo D-Y, Tian X, Lin H-P, et al. Niacin receptor GPR109A inhibits insulin secretion and is down-regulated in type 2 diabetic islet beta-cells. *Gen Comp Endocrinol*. 2016;237:98-108.
- Zafir B, Jain M. Lipid-lowering therapies, glucose control and incident diabetes: evidence, mechanisms and clinical implications. *Cardiovasc Drugs Ther*. 2014;28:361-377.
- Abel ED. Glucose transport in the heart. *Front Biosci*. 2004;9:201-215.
- Huang B, Wu P, Bowker-Kinley MM, Harris RA. Regulation of pyruvate dehydrogenase kinase expression by peroxisome proliferator-activated receptor- α ligands, glucocorticoids, and insulin. *Diabetes*. 2002;51:276-283.

32. van de Weijer T, Phielix E, Bilet L, et al. Evidence for a direct effect of the NAD⁺ precursor acipimox on muscle mitochondrial function in humans. *Diabetes*. 2015;64:1193-1201.
33. Lewis AJ, Miller JJ, McCallum C, et al. Assessment of metformin-induced changes in cardiac and hepatic redox state using hyperpolarized[1-13C]pyruvate. *Diabetes*. 2016;65:3544-3551.
34. Williamson DH, Lund P, Krebs HA. The redox state of free nicotinamide-adenine dinucleotide in the cytoplasm and mitochondria of rat liver. *Biochem J*. 1967;103:514-527.
35. Slart RH, Bax JJ, de Jong RM, et al. Comparison of gated PET with MRI for evaluation of left ventricular function in patients with coronary artery disease. *J Nucl Med*. 2004;45:176-182.

SUPPORTING INFORMATION

Additional Supporting Information may be found online in the Supporting Information section.

How to cite this article: Watson WD, Timm KN, Lewis AJ, et al. Nicotinic acid receptor agonists impair myocardial contractility by energy starvation. *The FASEB Journal*. 2020;34:14878–14891. <https://doi.org/10.1096/fj.202000084RR>